2011

Sensitization behaviour of 11-12% Cr AISI 409 stainless steel during low heat input welding

Cornelis Janise Van Niekerk
University of Pretoria

Madeleine du Toit
University of Wollongong, mdt@uow.edu.au

Publication Details

Van Niekerk, C. J. & Du Toit, M. (2011). Sensitization behaviour of 11-12% Cr AISI 409 stainless steel during low heat input welding. Journal of the South African Institute of Mining and Metallurgy, 111 (4), 243-256.

Sensitization behaviour of 11-12% Cr AISI 409 stainless steel during low heat input welding

Abstract
The study comprised of the investigation into the sensitization characteristics of AISI 409 titanium stabilized ferritic stainless steel during low heat input welding. AISI 409 is a fully ferritic stainless steel used in catalytic converters and tubing for automotive exhaust systems due to the supposition that sensitization does not occur during low heat input welding. Two plates of 2 and 4 mm were tested for sensitization during low heat input welding. The study confirmed that chromium carbide ($M_{23}C_6$) precipitation occurs on the grain boundaries in the heat-affected zone with consequent depletion of Cr adjacent to the grain boundaries during welding. In the 2 mm plate sensitization occurred in the heat input range of 0.1 kJ/mm to above 0.25 kJ/mm and in the 4 mm plate sensitization occurred in the heat input range of 0.2 to 0.9 kJ/mm. Ti stabilization is ineffective at the heat inputs used in this investigation due to the rapid cooling rate through the temperature region where TiC precipitates. The presence of N was found to be detrimental since it consumes Ti on cooling, forming TiN, effectively lowering the amount of Ti available for TiC formation during rapid cooling after welding. Annealing for 5 minutes at 725°C does not improve the sensitization characteristics of the welded plate. There is a linear increase in grain size as heat input increases. The resistance to pitting corrosion decreases in the sensitized, welded plate in the heat-affected zone adjacent to the fusion line of welding.

Keywords
sensitization, during, behaviour, heat, 409, stainless, aisi, steel, cr, welding, low, 12, input, 11

Disciplines
Engineering | Science and Technology Studies

Publication Details
Van Niekerk, C. J. & Du Toit, M. (2011). Sensitization behaviour of 11-12% Cr AISI 409 stainless steel during low heat input welding. Journal of the South African Institute of Mining and Metallurgy, 111 (4), 243-256.

Sensitization behaviour of 11–12% Cr AISI 409 stainless steel during low heat input welding

by C.J. van Niekerk* and M. du Toit*

Paper written on project work carried out in partial fulfilment of BEng Metallurgical Engineering

Synopsis

The study comprised of the investigation into the sensitization characteristics of AISI 409 titanium stabilized ferritic stainless steel during low heat input welding. AISI 409 is a fully ferritic stainless steel used in catalytic converters and tubing for automotive exhaust systems due to the supposition that sensitization does not occur during low heat input welding. Two plates of 2 and 4 mm were tested for sensitization during low heat input welding. The study confirmed that chromium carbide ($M_{23}C_6$) precipitation occurs on the grain boundaries in the heat-affected zone with consequent depletion of Cr adjacent to the grain boundaries during welding. In the 2 mm plate sensitization occurred in the heat input range of 0.1 kJ/mm to above 0.25 kJ/mm and in the 4 mm plate sensitization occurred in the heat input range of 0.2 to 0.9 kJ/mm. Ti stabilization is ineffective at the heat inputs used in this investigation due to the rapid cooling rate through the temperature region where TiC precipitates. The presence of N was found to be detrimental since it consumes Ti on cooling, forming TiN, effectively lowering the amount of Ti available for TiC formation during rapid cooling after welding. Annealing for 5 minutes at 725°C does not improve the sensitization characteristics of the welded plate. There is a linear increase in grain size as heat input increases. The resistance to pitting corrosion decreases in the sensitized, welded plate in the heat-affected zone adjacent to the fusion line of welding.

Keywords
AISI 409 ferritic stainless steel, sensitization, grain growth, resistance to pitting corrosion, low heat input welding.

Introduction

The weldability of AISI 409 is considered fair and in this paper its sensitization behaviour after gas tungsten arc welding (GTAW) was investigated. AISI 409 is a low carbon, 10.5 to 12 per cent Cr, Ti stabilized, ferritic stainless steel. It is used in applications such silencers, catalytic converters and tubing for automotive exhaust systems. It has the specified chemical composition limits as shown in Table I. Its melting temperature is in the range of 1 480–1 530°C[1].

AISI 409 is utilized in catalytic converters in automotive exhaust systems in favour of its good corrosion resistance, moderate price and the supposition that it has good resistance to sensitization during thermal cycles, thus replacing aluminized carbon steel. Gas metal arc welding (GMAW) is used in the manufacturing process. Due to the corrosive environment of the application of AISI 409 intergranular corrosion (IGC) has been detected in the heat-affected zone (HAZ) of weldments. The corrosive atmosphere in an exhaust system is mainly due to condensed water and exhaust gas containing Cl^-, SO_4^{2-}, SO^{3-}, CH_3COOH, CO_3^{2-} and HCO_3^- [2].

Figure 1 is a cross-section of the ternary Fe-Cr-C phase diagram. The steel considered here is designed to pass, on cooling, through the diagram to the right of the (δ + λ) loop, i.e. it remains fully ferritic from its melting temperature down to room temperature.

Although AISI 409 has a maximum carbon content of 0.03 per cent, Figure 1 is illustrative of the shape of the austenite and (austenite + ferrite) phase fields of the alloy. An increase in carbon content will enlarge these phases at the expense of ferrite, yet is compensated for by excess titanium (an excellent ferrite former when in solid solution), shifting the λ and (δ + λ) phase boundaries to the left of the diagram, which results in the fully ferritic (δ) matrix.

As a result of the absence of grain boundary austenite/martensite, AISI 409 undergoes grain growth in the heat-affected zones (HAZ) of weldments. As a consequence— in the as-welded state—it has poor toughness, fatigue and tensile properties[1,3].

The carbon and nitrogen contents are kept to a minimum to improve toughness, minimize sensitization of the steel and to maintain a ferritic structure. Consequently, ferritic stainless steels are not high-strength steels. In the annealed condition these steels have yield strengths in the order of 275-415 MPa[4].

AISI 409 is typically supplied in the annealed condition. Annealing is carried out between 700°C and 750°C[1]. During the annealing of titanium stabilized stainless

* *University of Pretoria.*

 SA ISSN 0038–223X/3.00 + 0.00. Paper received Mar. 2011; revised paper received Mar. 2011.

Table I

Specified chemical composition limits for grade AISI 409 (% by mass, balance Fe, single values are maximum levels)[1]

C	Si	Mn	P	S	Cr	Ni	N	Ti
0.03	1.00	1.00	0.04	0.02	10.5–11.70	0.05	0.03	0.18–0.75

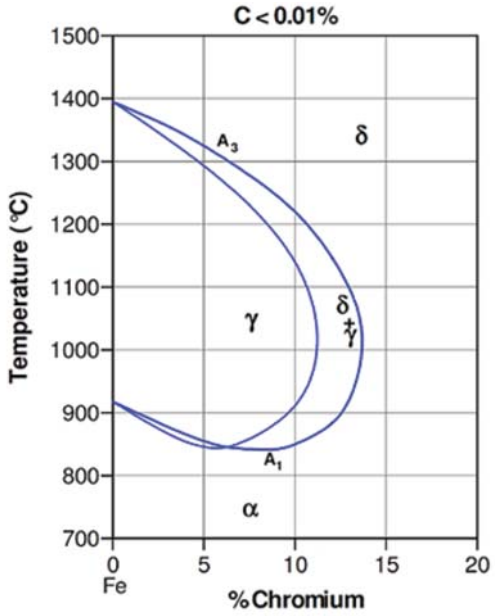

Figure 1 – Vertical section of the ternary Fe-Cr-C phase diagram for steels with Carbon content less than 0.01%[3]

steels in this temperature range the majority of carbon and titanium precipitate homogeneously throughout the matrix as highly stable titanium carbides (TiC), titanium nitrides (TiN), or carbo-nitrides (TiCN). This inhibits the precipitation of sensitizing chromium-rich carbides due to carbon's higher affinity for titanium when compared to chromium, i.e. titanium carbide precipitation requires a lower free energy (ΔG) to nucleate than chromium carbides. This effectively stabilizes the steel against intergranular corrosion caused by sensitization[3].

Austenitic consumables such as 308L, 309L and 316L are recommended as filler metals to improve the toughness of welds. In order to limit grain growth, it is generally considered beneficial to use minimum heat inputs during welding. Edge welds should be avoided. When welding e.g. lap joints, a maximum combined thickness of 3 mm should be maintained, i.e. 2 × 1.5 mm thickness on each plate being joined by welding[1,5].

Literature review

According to Kim *et al.*[2] sensitization to IGC can occur in AISI 409 specimens, aged in the temperature range of 400–600°C, which represents the sensitization nose of the time-temperature-sensitization (TTC) diagram at 600°C, especially after welding. Kim *et al.*[6] also found that higher chromium contents decrease the extent of IGC but does not prevent it.

Various models have been proposed for the sensitization of stainless steels. Sensitization by means of chromium depletion due to the precipitation of chromium-rich carbides is the most widely agreed upon[2,7]. According to this theory carbides of the type $M_{23}C_6$ or rather $(Fe,Cr)_{23}C_6$ precipitate intergranularly where a surface is available which will lower the energy required for nucleation of the precipitate. This results in chromium depletion of the matrix directly adjacent to the grain boundaries on which the precipitates form. The steel becomes susceptible to intergranular corrosion when the chromium content in the affected matrix adjacent to the grain boundary area falls below that required for passivation (in the order of 11.5 per cent Cr). It reduces the corrosion resistance of the steel in the vicinity of the grain boundaries and the steel may suffer preferential attack when exposed to a corrosive environment as aforementioned. In general, chromium-rich $M_{23}C_6$ precipitates form in ferrite in the temperature range of 550–850°C[8].

Carbon solubility is lower in ferrite than in austenite due to a much more densely packed body-centred cubic (BCC) crystal structure which has less interstitial spaces than the austenitic face-centred cubic (FCC) lattice. A consequence of this structure is that carbon has a much faster diffusivity in ferrite than in austenite. This allows sensitization to occur more easily and rapidly than in any other stainless steel even when subjected to a rapid quench after welding[3,8].

Due to the high diffusion rates in ferrite, carbides form rapidly during annealing. In the as-supplied condition (fully annealed) these steels therefore contain carbides, but are in the fully de-sensitized condition due to chromium diffusion into any Cr-depleted zones during heat treatment. These steels can only resensitize by being heated to a temperature above the carbide dissolution temperature (± 950°C) followed by rapid cooling to prevent carbon back-diffusion.

A lowering of the carbon content to below even 0.01 per cent does not prevent sensitization in ferritic stainless steels; therefore, stabilizing agents are added such as Ti and Nb. These stabilizers are added in sufficient quantities to combine with most of the carbon in the steel. These elements minimize the formation of $M_{23}C_6$ carbides but they also reduce the temperature at which these carbides undergo dissolution[9].

During annealing, Ti stabilized ferritic stainless steel such as AISI 409 forms titanium carbides (TiC), which is stable at high temperatures. TiC precipitation requires a lower driving force than $M_{23}C_6$ and therefore Ti acts as a stabilizsing agent against sensitization, arresting any chromium carbides that would subsequently form on cooling in an otherwise non-stabilized stainless steel. Excess carbon is consumed in the supersaturated ferrite matrix by precipitating TiC at temperatures higher than the $M_{23}C_6$ precipitation range, hence no carbon is available to form carbides with chromium at lower temperatures[10].

Equations [1] and [2] have been established in literature for the determination of the appropriate Ti content for successful stabilization of 12 per cent Cr Steels, as follows[11].

$$\%Ti > 4 * (\%C + \%N) \quad [1]$$

$$\%Ti > 0.08\% + 8 * (\%C + \%N) \quad [2]$$

These equations promote over-stabilization.

During high heat input welding chromium back-diffusion in ferrite grains plays an important role in mitigating sensitization. The sensitized areas are given time to 'heal' when chromium from the grain interiors diffuse into the depleted and sensitised zones until the per cent Cr is again above the necessary level for passivation, restoring the corrosion resistance which is due to the chromium oxide film Cr_2O_3[12].

Four modes of HAZ sensitization have been identified in 12 per cent Cr steel, most of them involving dual phase ($\gamma + \delta$) stainless steel where the austenite in the steel transform to martensite during the rapid cooling rates associated with welding. Mode 3 sensitization corresponds to the sensitization found in titanium stabilized stainless steels with a high Kaltenhauser ferrite factor (KFF) or fully ferritic stainless steel such as AISI 409[11,12,13].

Mode 3 sensitization occurs in the coarse-grained region directly adjacent to the fusion line. In dual phase ferritic stainless steels this region consists mostly of ferrite-ferrite grain boundaries and in the case of AISI 409, fully ferritic grains. The absence of austenite (which acts as a carbon sink) in this region and the low solubility of carbon in ferrite, causes the ferrite matrix to be supersaturated with carbon. Chromium-rich carbides precipitate extensively along grain boundaries in the initial stages of cooling after welding. Mode 3 can therefore occur along the grain boundaries of the high temperature heat-affected zone (HTHAZ) of weldments during low heat input, single-pass weld with a fast subsequent cooling rate, shallow weld toe cusps and arc strikes. The rapid thermal cycle of low heat input welding does not allow for chromium back-diffusion to affected areas from the grain interiors and the HAZ contains a continuous sensitized network of ferrite-ferrite grain boundaries down to room temperature[12,13,14].

The chromium depleted or sensitized sites will undergo anodic dissolution in a corrosive environment, which results in intergranular corrosion (IGC). In the presence of considerable operating and residual stresses this kind of corrosive attack is usually initiated as pitting corrosion. Individual pits eventually link up, resulting in intergranular stress corrosion cracking (IGSCC)[11].

Experimental procedure

Alloy composition

Two plates of AISI 409 of different thickness (2 and 4 mm) were used in this investigation, as the sensitization behaviour is both a function of plate thickness and chemical composition. Tables II and III gives the specific chemical compositions of these plates.

Welding procedure

Autogenous (bead on plate welds without filler metal) welding was performed on both plates using gas tungsten arc welding (GTAW) with negative electrode polarity. Pure welding-grade argon shielding gas at a flow rate of 15 ℓ/min was used.

The heat input of the welds on the 2 and 4 mm plates were range of 0.1–0.25 kJ/mm and 0.1–1.0 kJ/mm respectively.

Equation [3] was used to calculate the heat input (*HI*) of welding for each respective weld that was investigated. It incorporates the welding parameters used where *V* is the arc voltage, *I* is the welding current (A), ν is the travel speed of welding (mm/s) and *q* is the power or heat flux (W).

$$HI = \frac{\eta VI}{v} = q/v \quad [3]$$

The average arc efficiency (η) was estimated at 47.5 per cent which lies close to the upper limit normally stipulated for GTAW which is in the range of 22 to 48 per cent[15]. Tables IV and V lists the welding parameters selected to produce the desired heat inputs of welding.

Sensitization testing

To test for sensitization the ASTM Standard Practices for Detecting Susceptibility to Intergranular Attack in Ferritic Stainless Steels (A 763–93) were used on both the 2 and 4 mm thick plates after welding[16].

Practice W requires a 10% oxalic acid etch followed by investigation using a metallurgical microscope. Etching was carried out at 1 A/cm2 for 1.5 minutes. It reveals the presence

Table II

Chemical composition of the 2 mm thick plate of AISI 409 (% by mass, balance Fe)

C	Si	Mn	P	S	Cr	Mo	Ni	Al	Ti	Nb	Cu	V
0.03	0.61	0.52	0.03	<0.001	11.40	0.02	0.13	0.01	0.19	<0.002	0.11	0.07

Table III

Chemical composition of the 4 mm thick plate of AISI 409 (% by mass, balance Fe)

C	S	P	Mn	Si	Cu	Ti	Mo	Cr	Ni	Al	Nb	V	N	B
0. 011	0.0005	0.23	0.54	0.6	0.06	0.187	0.015	11.43	0.11	0.008	0.001	0.09	0.0135	0.0005

Table IV

Heat input range of weldments on the 2 mm thick plate

Weld	Welding current (A)	Arc potential (V)	Welding speed (mm/s)	Power (W)	Heat input (kJ/mm)
1	41	15.5	3.2	0.30	0.095
2	50	15	3.2	0.36	0.112
3	55	14	2.8	0.37	0.131
4	60	16	3.2	0.46	0.143
5	65	14	2.8	0.43	0.155
6	70	15.5	3.2	0.52	0.162
7	81	16	2.8	0.62	0.221
8	99	15	2.8	0.71	0.253

Table V

Heat input range of weldments on the 4 mm thick plate

Weld	Welding current (A)	Arc potential (V)	Welding speed (mm/s)	Power (W)	Heat input (kJ/mm)
1	50	15	3.0	0.36	0.12
2	78	16	3.0	0.60	0.20
3	119	17	3.0	0.96	0.32
4	138	18	3.0	1.20	0.40
5	164	19	3.0	1.50	0.50
6	199	19	3.0	1.80	0.60
7	207	21	3.0	2.10	0.70
8	227	22	3.0	2.40	0.80
9	257	22	3.0	2.70	0.90
10	272	23	3.0	3.00	1.00

of chromium carbides by removing any carbide present on the surface area of the microstructure exposed to the oxalic acid solution during etching. Therefore, any continuous and darkened network of grain boundaries is an indication of the presence of chromium-rich carbides.

Practice Z requires the samples to be boiled for 24 hours in a copper-copper sulphate-16% sulphuric acid solution. The samples are to be in contact with copper clippings to induce a galvanic effect between the steel and the copper to enhance the corrosion effect of the acid on the steel. Previous work cited the parameters of the test too severe[8]. For this reason the total time of boiling was reduced to 4 hours and the sulphuric acid was used at a concentration of 6% H_2SO_4. The samples were then analysed and scanning electron microscope (SEM) images were taken. Practice Z reveals the chromium depleted zones adjacent to grain boundaries. Energy dispersive spectroscopy (EDS) was done after Practice Z on titanium carbides, titanium nitrides and chromium carbides.

Annealing

A sample from the 4 mm thick plate, welded at a heat input of 0.5 kJ/mm was annealed at a temperature of 725°C with a holding time of 5 minutes. The sample was then subjected to ASTM practice Z to determine the effect of annealing on the extent of chromium back diffusion into Cr-depleted grain boundaries.

Grain size estimation

The average grain diameter of the HAZ was determined for each sample of the 4 mm thick plate, welded at the heat inputs stated in Table V, with the Heyn Lineal Intercept Procedure specified in the ASTM Standard Test Methods for Determining Average Grain Size (E 112–96)[17].

Corrosion tests

The corrosion, pitting and protection potentials were established for the unwelded (as-received) plate and a sample welded at a heat input of 0.4 kJ/mm using the Standard ASTM practice G 150–99[18]. The corrosion test was carried out in an Avesta Cell (an electrochemical cell which limits the occurrence of crevice corrosion) with a 3.5% NaCl solution, deaerated for 30 minutes with nitrogen gas prior to testing. A Ag/AgCl reference electrode was used. The results obtained from the corrosion tests were compared to establish the influence of sensitization and welding on the corrosion characteristics of the steel.

Heat flow modelling

In order to quantify the effect of heat input on the thermal cycle, Rosenthal's heat flow equations of a moving point heat source were used to model conduction driven heat flow in the heat-affected zones of the 4 mm welded samples 100 μm from the fusion line[19].

Phase stability regions simulated in FactSage™ software

The thermal cycle of welding is not an equilibrium process but equilibrium calculations give a good indication of what phases are stable at specific temperatures. The specific chemical composition of the 4 mm steel was used to predict a pseudo equilibrium phase stability diagram using FactSage™ software. The same was done with the titanium content halved. Temperatures from these diagrams were used to predict the time spent within each phase stability region during cooling after welding, using the Rosenthal equations. FactSage™ was also used to predict, at equilibrium, the weight percentage of TiN and TiC that would precipitate during cooling of the plate from the molten state.

XRD

In order to analyse the precipitates, five welding beads, welded in the region where sensitization was found to be most prolific, were dissolved in a solution of 35% HCl. The solution was then filtered using glass fibre filter paper with an average aperture diameter of 0.7 μm. The filtered product was rinsed with distilled water and acetone to achieve agglomeration of the filtrate and air dried before XRD analysis.

Results and discussion

Figures 2 and 3 shows the difference in the microstructures (4 mm samples) of the as-received and welded plates. The sample of figure 3 was welded at a heat input of 0.4 kJ/mm and both were etched with 50 ml HNO_3, 50 ml HCl, and 50 ml water by submersion for 90 seconds.

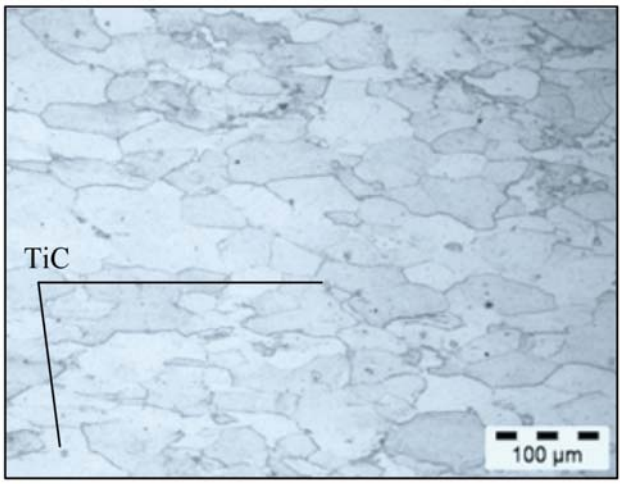

Figure 2–Typical AISI 409 microstructure in the as-received condition (etched with 50 ml HNO_3, 50 HCL and 50 ml water for 90 seconds). TiC precipitates are also visible

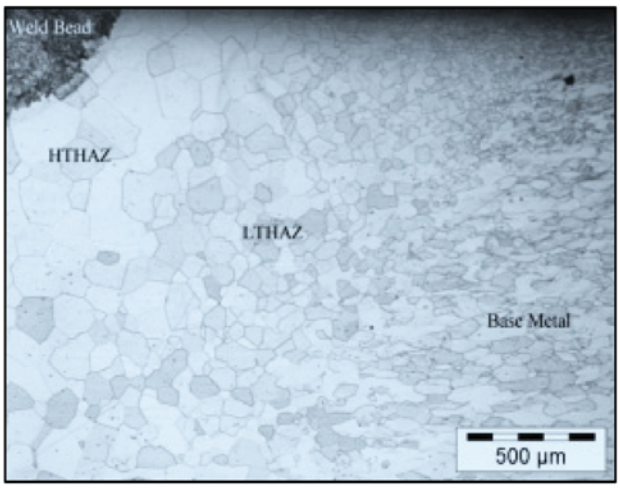

Figure 3–Four distinct phases present on the microstructure after welding (4 mm plate welded at a heat input of 0.4 kJ/mm and etched with 50 ml HNO_3, 50 ml HCL and 50 ml water)

2 mm thick plate after GTAW

Practice W

Figures 4–7 are optical micrographs taken with an optical microscope of the 2 mm thick 409 steel samples, welded at the heat inputs listed in Table IV, subjected to ASTM Practice W.

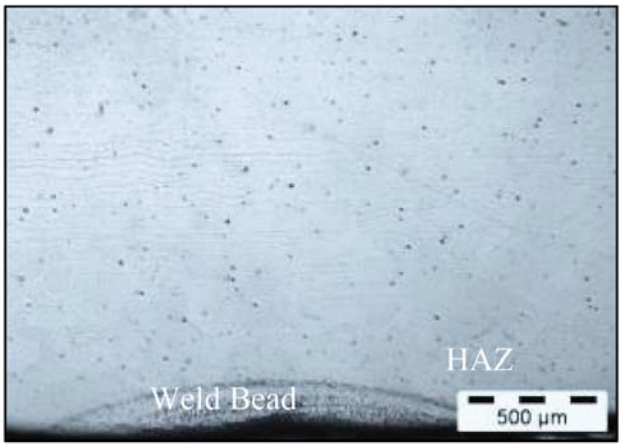

Figure 4—2 mm thick AISI 409 welded at a heat input of 0.095 kJ/mm (Practice W)

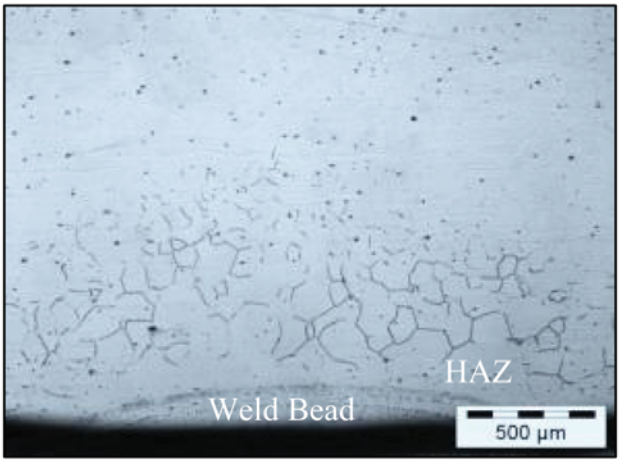

Figure 5—2 mm thick AISI 409 welded at a heat input of 0.11 kJ/mm (Practice W)

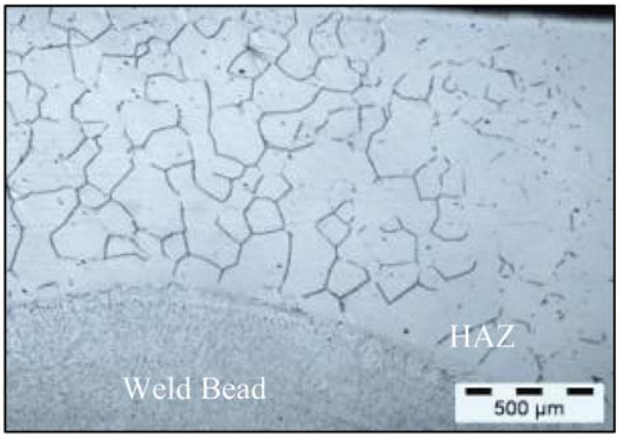

Figure 6—2 mm thick AISI 409 welded at a heat input of 0.14 kJ/mm (Practice W)

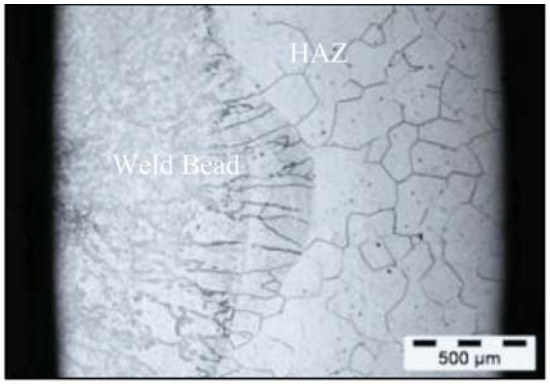

Figure 7—2 mm thick AISI 409 welded at a heat input of 0.15 kJ/mm (Practice W)

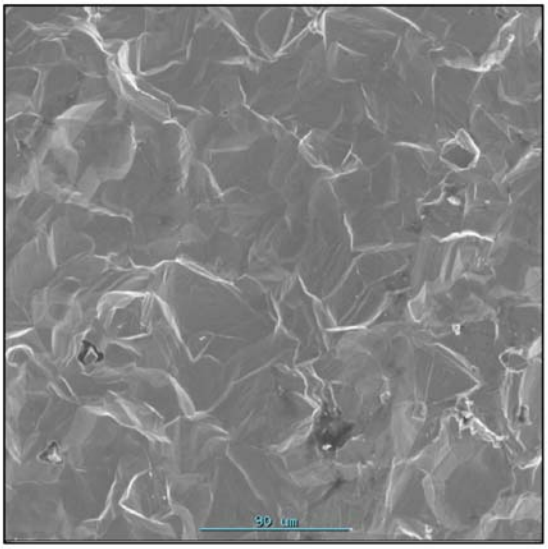

Figure 8—Unsensitized microstructure of control sample subjected to modified Practice Z

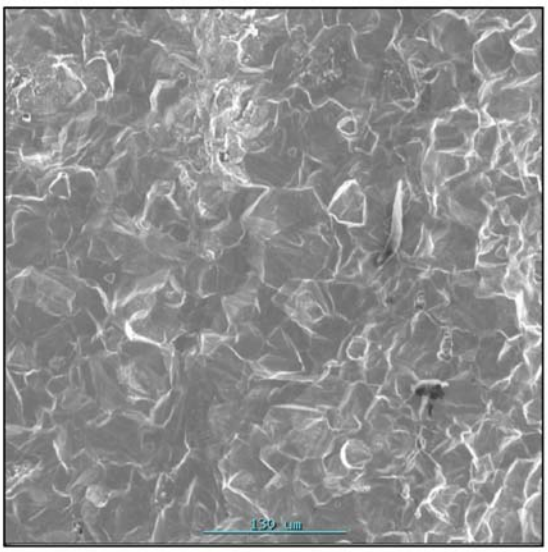

Figure—9 HAZ of the 2 mm thick AISI 409 welded at a heat input of 0.095 kJ/mm (Modified Practice Z)

Figure 4 (welded at a heat input of 0.095 kJ/mm) shows some grain boundaries outlined by Practice W, yet no grain boundaries reveal the presence of chromium carbide precipitation ($M_{23}C_6$) in the HAZ. Figures 5–7 reveal the presence of intergranular chromium carbide precipitates in the high temperature heat-affected zone (HTHAZ) closer to the weld bead. Chromium carbides are indicated by darkened grain boundaries where the carbides were attacked (and dissolved) by Practice W.

Practice Z

Figures 8–12 are photomicrographs taken on a scanning electron microscope (SEM) of the HAZ of the welded 2 mm samples that were subjected to the modified ASTM Practice Z. Figure 8 is an unwelded and unsensitised control sample added to the test for comparative purposes.

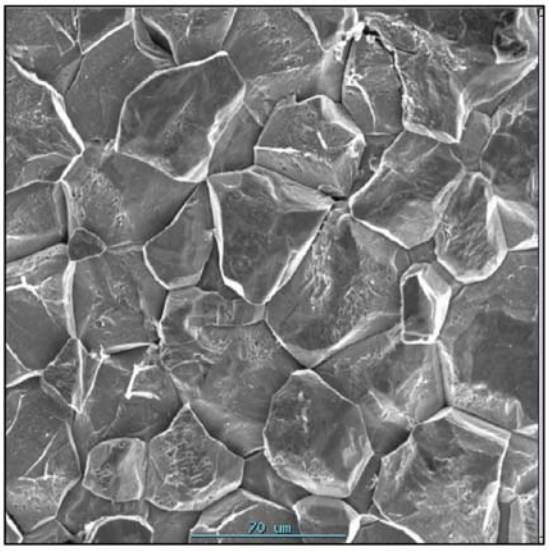

Figure 10—HAZ of the 2 mm thick AISI 409 welded at a heat input of 0.11 kJ/mm (Modified Practice Z)

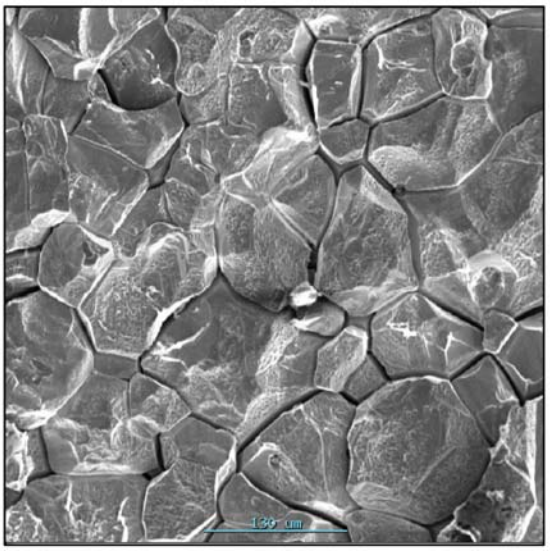

Figure 11—HAZ of the 2 mm thick AISI 409 welded at a heat input of 0.14 kJ/mm (Modified Practice Z)

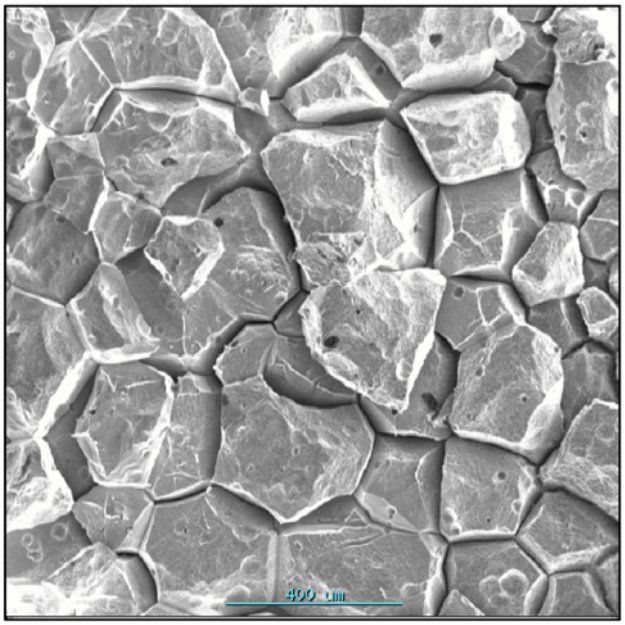

Figure 12—HAZ of the 2 mm thick AISI 409 welded at a heat input of 0.25 kJ/mm (Modified Practice Z)

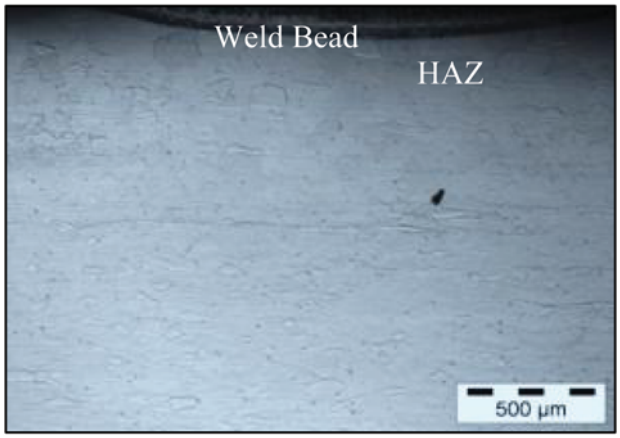

Figure 13—4 mm thick AISI 409 welded at a heat input of 0.1 kJ/mm (Practice W)

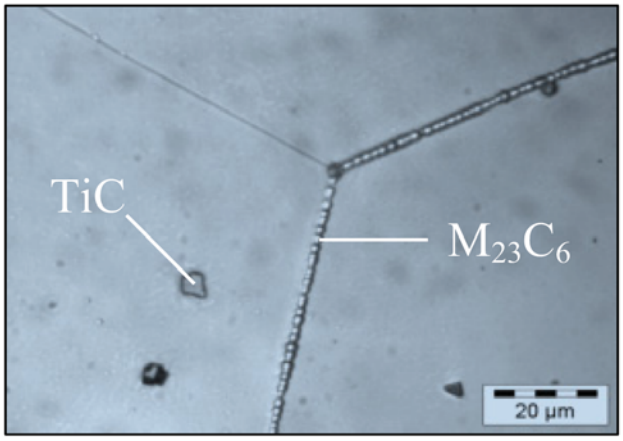

Figure 14—4 mm thick AISI 409 welded at a heat input of 0.20 kJ/mm at higher magnification (Practice W)

Figure 9 compares well with Figure 8 in that no grain boundary ditching is evident. None of the areas adjacent to the grain boundaries experienced anodic dissolution during Practice Z. This is an indication of the absence of chromium depletion in these areas, corresponding to Figure 4.

Figures 9–12 show extensive grain boundary ditching. It is evident that the areas adjacent to the grain boundaries were depleted of chromium where chromium carbides precipitated intergranularly. Where the Cr content dropped below the concentration required for passivation (about 11.5 per cent) these areas underwent anodic dissolution during the implementation of the modified Practice Z.

Cooling through the temperature range where Cr atoms are mobile in the ferrite matrix is too rapid for Cr from within the grain interiors to diffuse back to those areas depleted of Cr.

4 mm thick plate after GTAW

Practice W

Figures 13–18 are optical micrographs taken with an optical microscope of the 4 mm thick 409 plate. These samples were welded at the heat inputs given in Table V, subjected to ASTM Practice W.

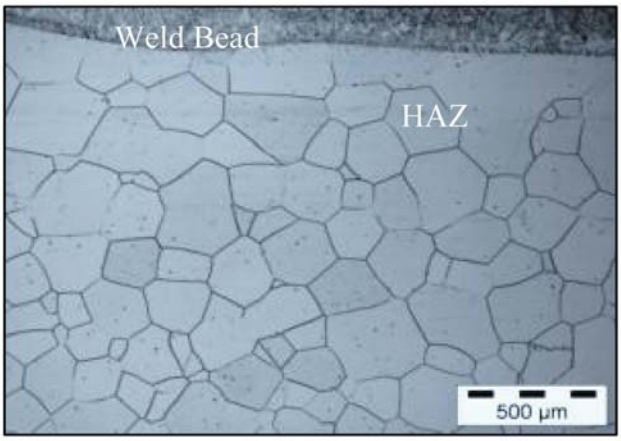

Figure 15—4 mm thick AISI 409 welded at a heat input of 0.50 kJ/mm (Practice W)

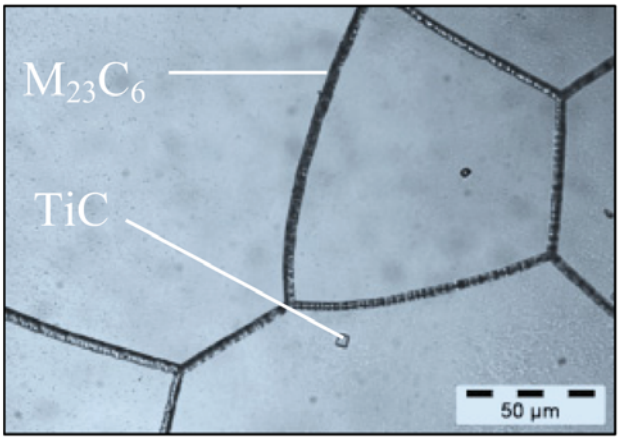

Figure 16—4 mm thick AISI 409 welded at a heat input of 0.60 kJ/mm at higher magnification (Practice W)

Evident from Figure 13 no chromium carbides precipitated at a heat input of 0.1 kJ/mm. In the heat input range of 0.2–0.9 kJ/mm, chromium carbides precipitated intergranularly in the heat-affected zones. At a heat input of 1.0 kJ/mm there is again an absence of intergranular chromium carbides. The absence of carbides at a heat input of 0.1 and 1.0 kJ/mm is ascribed to the cooling rate. At a heat input of 0.1 kJ/mm (Figure 18) the cooling rate is too rapid for carbide precipitation and at 1.0 kJ/mm the cooling rate is such that enough time is allocated in the thermal cycle of welding to allow for titanium stabilization to be effective.

Modified practice Z

Figures 19–23 are micrographs taken on the SEM of the HAZ of the welded samples of the 4 mm thick plate after the application of the modified Practice Z, welded at the respective heat inputs stated in Table V.

Figures 19 (heat input of 0.1 kJ/mm) and 23 (heat input of 1.0 kJ/mm) shows no ditching of the grain boundaries, which indicates that no chromium depletion adjacent to grain boundaries took place which is in turn indicative of no carbides ($M_{23}C_6$) precipitated on the grain boundaries. This corresponds to Figures 13 and 18 of Practice W of samples

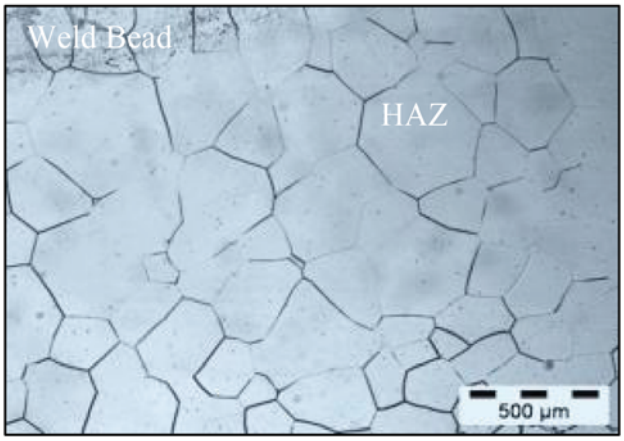

Figure 17—4 mm thick AISI 409 welded at a heat input of 0.70 kJ/mm (Practice W)

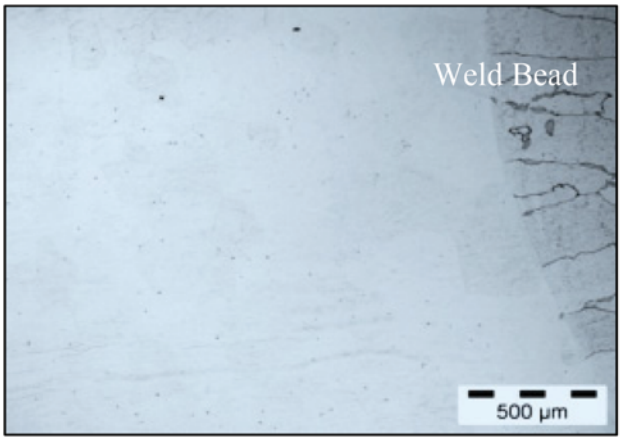

Figure 18—4 mm thick AISI 409 welded at a heat input of 1. 0 kJ/mm (Practice W)

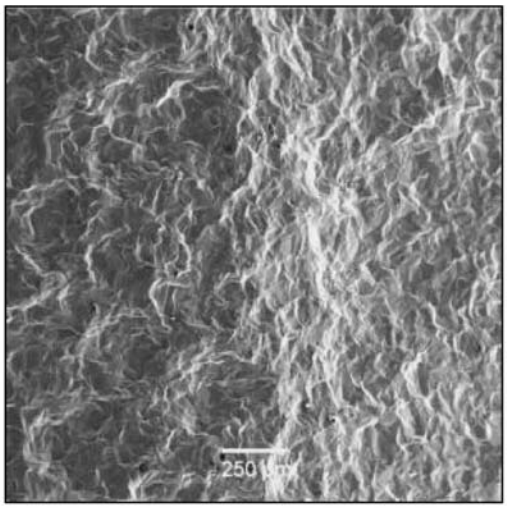

Figure 19—4 mm thick AISI 409 welded at a heat input of 0.10 kJ/mm (Modified Practice Z)

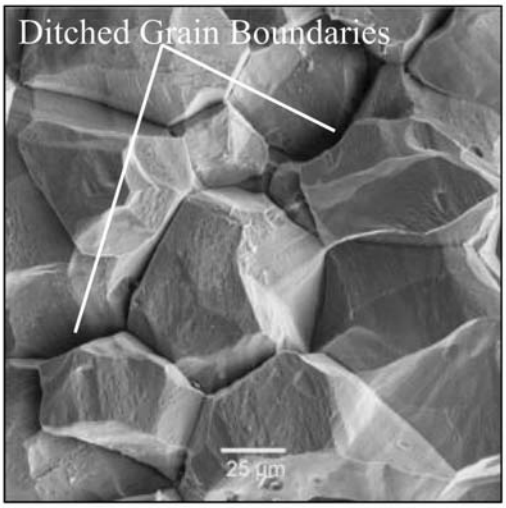

Figure 20—HAZ of 4 mm thick AISI 409 welded at a heat input of 0.20 kJ/mm at a larger magnification (Modified Practice Z)

Figure 21—4 mm thick AISI 409 welded at a heat input of 0.32 kJ/mm (Modified Practice Z)

welded at the same heat input levels. Also at higher heat input levels and consequent slower cooling rates, chromium back diffusion plays a role in healing the areas that did indeed undergo chromium depletion due to carbide precipitation. Figures 20–22 shows extensive grain boundary ditching where the area adjacent to the grain boundaries were depleted of chromium below the level necessary for passivation.

Annealing after welding of 4 mm thick AISI 409 plate

A sample, welded at 0.5 kJ/mm that revealed carbide precipitation through Practice W and chromium depletion of the areas adjacent to the grain boundaries through the modified Practice Z, was annealed after welding at a temperature of 725°C for 5 minutes. The sample was air cooled and subjected to the modified Practice Z, to investigate the extent of chromium back diffusion in the annealing temperature range. Figures 24 and 25 were taken after the modified Practice Z on the SEM. Figure 24 is an electron back-scattered image of the HAZ.

From Figures 24 and 25 it is evident that annealing at these conditions is not sufficient to induce chromium back-diffusion successfully as sensitization occurs in the welding bead and chromium depletion is still prevalent within the HAZ. A double annealing treatment, i.e. two annealing cycles at 725°C for 5 minutes each with cooling in between, may be beneficial.

Chemical analyses on TiC, TiN and $M_{23}C_6$

Figures 26 and 27 show titanium carbides (TiC) and titanium nitrides (TiN) that were observed on the microstructures of the welded 4 mm thick plate after the application of Practice W and the modified Practice Z respectively.

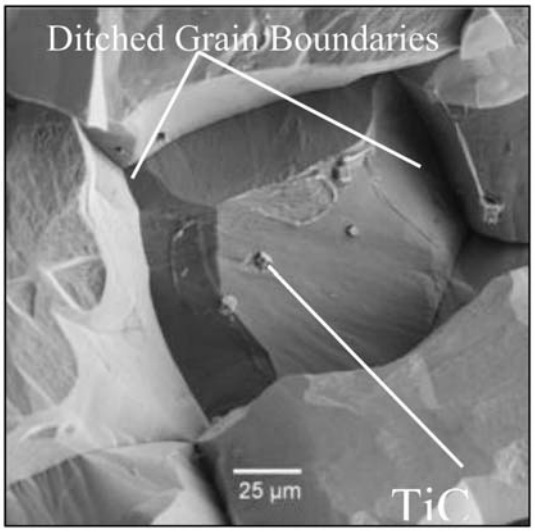

Figure 22—HAZ of 4 mm thick AISI 409 welded at a heat input of 0.50 kJ/mm at a larger magnification (Modified Practice Z)

Figure 23—4 mm thick AISI 409 welded at a heat input of 1.0 kJ/mm (Modified Practice Z)

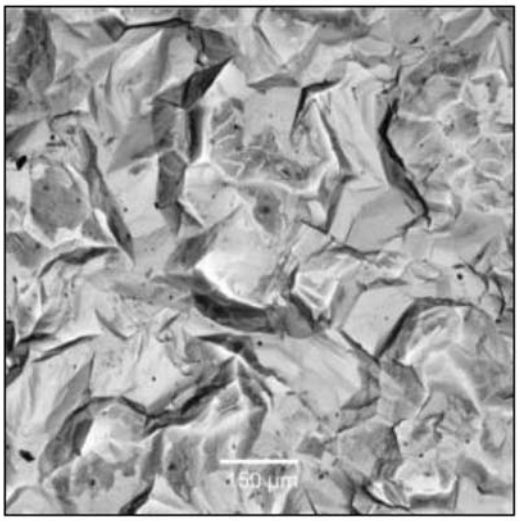

Figure 24—Electron back-scattered micrograph of the HAZ of a 4 mm thick AISI 409 plate welded at a heat input of 0.50 kJ/mm and annealed at 725°C for 5 minutes (Modified Practice Z)

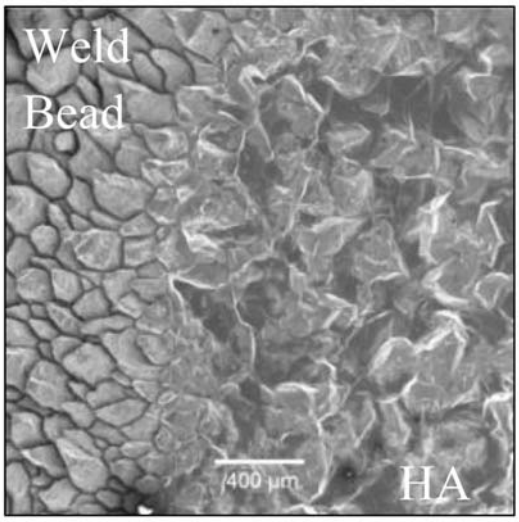

Figure 25—4 mm thick AISI 409 welded at a heat input of 0.50 kJ/mm and annealed at 725°C for 5 minutes showing sensitization of the welding bead (Modified Practice Z)

Titanium carbides appear as cubic precipitates varied in size and at random positions through the ferrite grains and on some grain boundaries. TiC also nucleates on already existing titanium containing precipitates like TiN, which nucleates and reaches stability before TiC during cooling. This is evident in Figures 28 and 29 where an EDS was performed on two different points on such a precipitate.

In Figure 29 it is apparent that the dark region in the centre of the cubic precipitate contains nitrogen and the light outer region contains carbon. XRD confirmed the presence of TiN and TiC in the weld bead and heat-affected zones of the welded samples.

An EDS scan was performed on a chromium carbide found along a grain boundary in the HAZ of a sample that was subjected to the modified Practice Z. The particle is shown in Figure 30 and the EDS in Figure 31.

Phase stability regions simulated in FactSage™ software

A phase stability diagram, Figure 32, showing the regions where the phases of interest to this study are stable during equilibrium cooling at varying chromium contents was simulated using FactSage™ software. The diagram is based on the specific chemical composition as given in Table III.

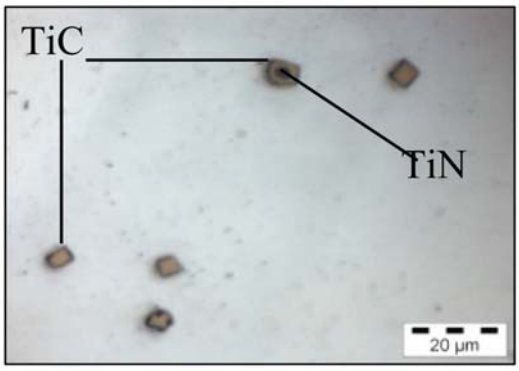

Figure 26—TiC and TiN in ferrite grains after Practice W (weld heat input—0.6 kJ/mm)

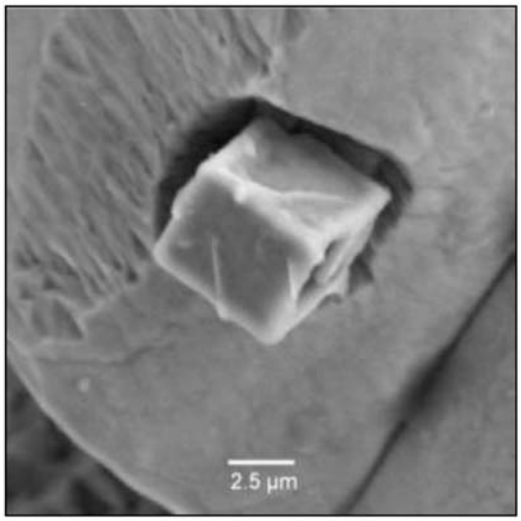

Figure 27—TiC and TiN in ferrite grains after modified Practice Z (weld heat input—0.4 kJ/mm)

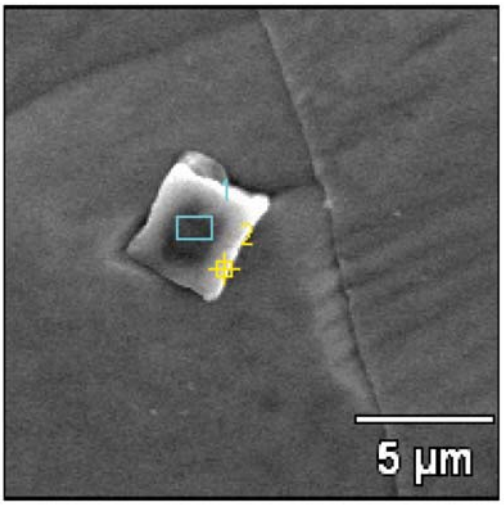

Figure 28—TiC and TiN in ferrite grains after Practice Z (weld heat input—0.8 kJ/mm)

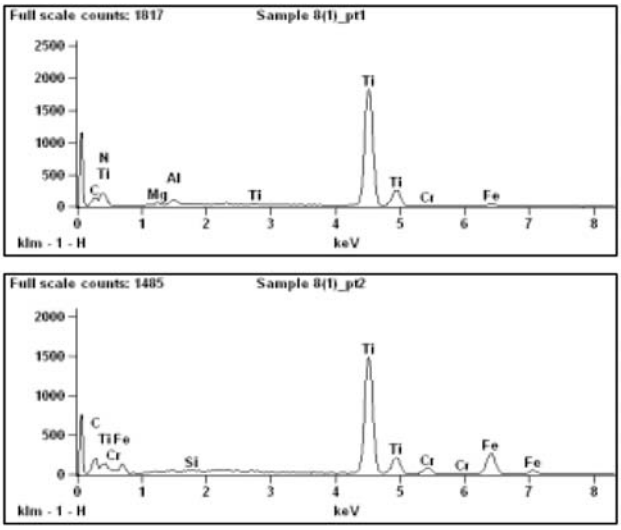

Figure 29—TiC and TiN EDS on SEM after Practice Z (weld heat input—0.8 kJ/mm)

Figure 30—$M_{23}C_6$ on ditched grain boundary after Practice Z (weld heat input—0.8 kJ/mm)

According to Figure 32, AISI 409 with Cr content of 11.4 per cent will solidify from the liquidus temperature as ferrite and TiN at a temperature just above 1 510°C followed by the formation of TiC at temperatures below 1 150°C. This structure remains stable down to room temperature, and suggests that, under equilibrium cooling conditions, the steel contains enough Ti to prevent sensitization, hence no chromium carbide precipitation is predicted.

At the non-equilibrium cooling conditions of the welding thermal cycle, the work piece cools too rapidly for Ti stabilization to be effective. This was simulated in FactSage™ by halving the Ti content of the original chemical composition in the equilibrium diagram of Figure 33.

The formation of chromium carbides is evident in Figure 33 with ineffective titanium stabilization.

Pardo *et al.*[20] found that the general equations used to predict the wt% Ti required for successful stabilization (Equations [2] and [3]) is inadequate at non-equilibrium cooling to prevent the formation of chromium rich $M_{23}C_6$. This is due to TiN formation and rapid cooling at the elevated temperatures where TiC becomes stable in the matrix and start to precipitate. On the phase diagram of Figure 32 it is shown that, on cooling, TiN formation occurs before TiC formation which corresponds well to the micrographs of Figures 26 and 28 where TiC was observed to have nucleated on existing TiN precipitates. The formation of TiN consumes Ti, which results in more C available for the formation of $M_{23}C_6$, also evident in Figure 33.

Figure 34 is a simulation (using Factsage™) of the amounts of TiN and TiC that would form under equilibrium cooling conditions for the chemical composition of the 4 mm thick plate stated in Table III.

Heat flow modelling for non-equilibrium cooling after welding

Using Rosenthal's theory on moving point heat sources, it was possible to model the heat flow of the weld thermal cycle of the 4 mm plate at the various heat inputs. A point was selected at 0.1 mm away from the fusion line at which to model the heat flow, the point falls within the high temperature heat-affected zone of each welded sample. Figure 35 shows the difference in cooling rate resulting from the maximum and minimum heat inputs used in this investigation.

Evident from Figure 35, as the heat input increases, the cooling rate decreases. This allows more cooling time through the temperature range where TiC precipitates, thus less $M_{23}C_6$

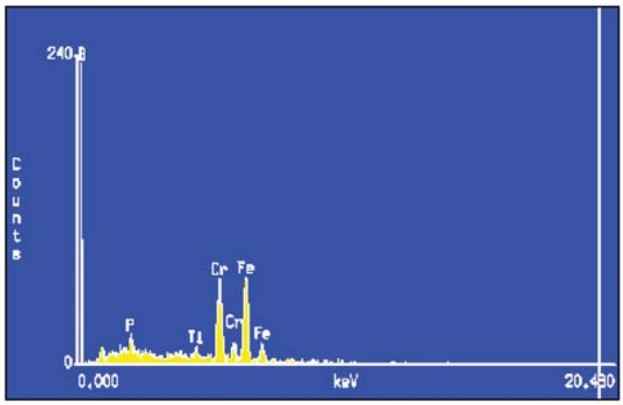

Figure 31—$M_{23}C_6$ EDS on SEM after Practice Z (weld heat input—0.4 kJ/mm)

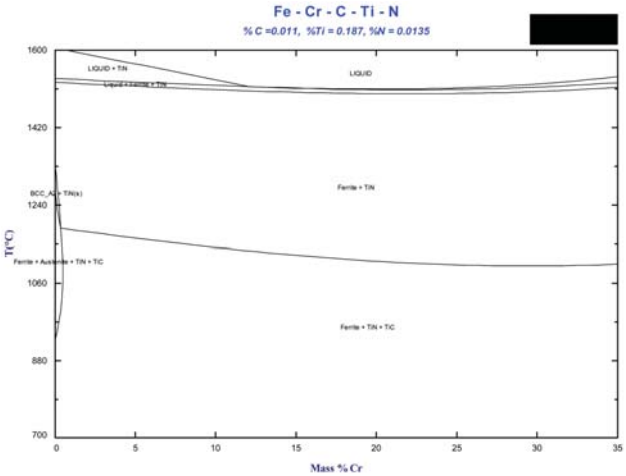

Figure 32—Phase stability diagram for AISI 409 simulated using FactSage™ software

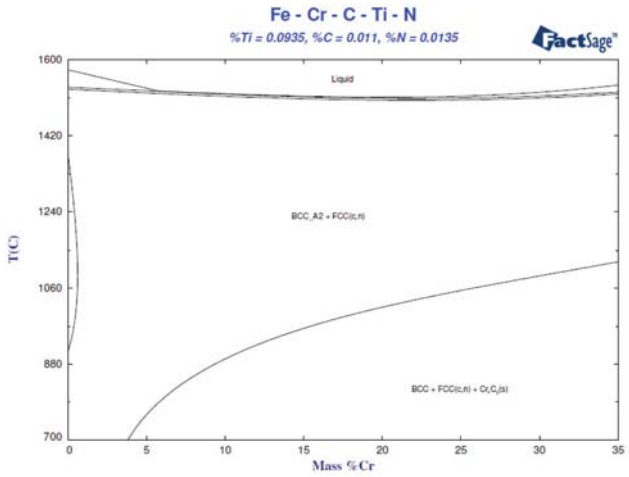

Figure 33—Phase stability diagram for AISI 409 simulated using FactSage™ software at half the titanium content

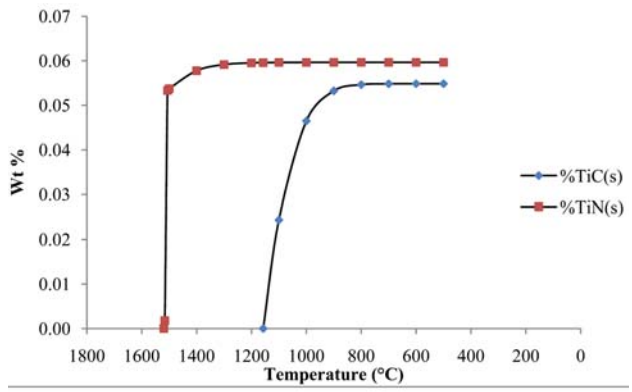

Figure 34—Wt% TiN and TiC at equilibrium cooling as a function of cooling temperature simulated using FactSage™ software

form on cooling. The slower cooling rate also allows more time for Cr back-diffusion to the areas adjacent to grain boundaries that have been depleted of Cr and passivity is restored where the Cr content have dropped to such an extent that passivity was lost.

By using Rosenthal's theory in conjunction with the phase stability diagrams simulated in FactSage™ the amount of time spent on cooling in each phase stability region could be estimated for each respective heat input weld. The temperature range in which TiC is stable on cooling was taken to be 750–1 150°C and that in which $M_{23}C_6$ is stable was taken to be 550–925°C. This resulted in the two respective curves of Figure 36.

Figure 36 shows that the time spent in the region where $M_{23}C_6$ precipitates is virtually double the time spent in the region where TiC precipitates. The holding times in the region where TiC becomes stable is evidently not enough for Ti to successfully combine with all of the free carbon in the matrix at fast cooling rates. Due to carbon's rapid diffusion rate through the matrix at elevated temperatures enough C atoms pile up in the grain boundaries where Cr is removed from the adjacent areas to form stable chromium carbides.

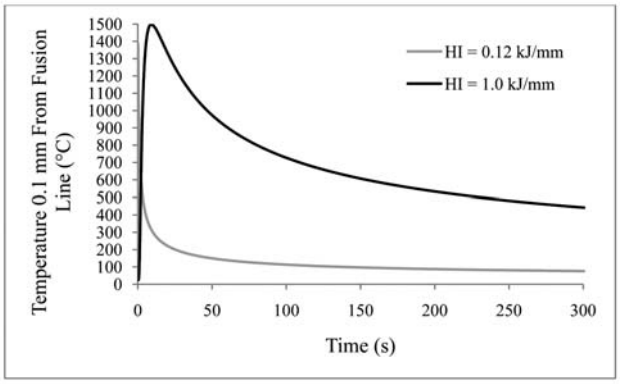

Figure 35—Calculated temperature cycles experienced by the high temperature heat-affected zone at a point located 100 µm from the fusion line for heat inputs of 0.1 kJ/mm and 1.0 kJ/mm and plate of thickness 4 mm

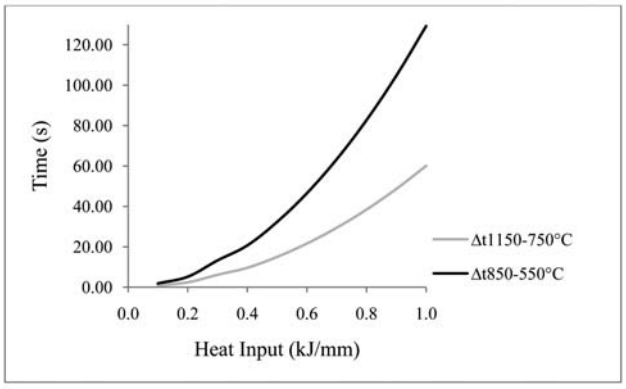

Figure 36—Calculated amount of time spent in TiC and $M_{23}C_6$ stability range on cooling after welding for samples 4 mm thick plate welded at heat inputs ranging from 0.1 kJ/mm to 1.0 kJ/mm

Grain size estimation

The average grain size of the HTHAZ of each welded sample of the 4 mm plate was determined over the range of heat inputs using the Heyn Lineal Intercept Procedure. The samples prepared for the measurement of grain size were etched by submersion in a 50 ml HNO_3, 50 ml HCL and 50 ml water solution for 2 minutes.

Figure 37 shows the mean lineal intercept, or average grain diameter, as a function of the heat input of welding. It can be seen that as the heat input increases the average grain diamater increases as a linear function of the heat input. Indicated on Figure 37 is the per cent relative accuracy.

On welding AISI 409 at low heat inputs a compromise needs to be reached between sensitization and the amount of grain growth that can be tolerated. Figure 38 shows the average grain boundary area within a volume of 1 mm³ of the HTHAZ that was determined using Equation [4].

$$S_v = \frac{2}{\ell} \qquad [4]$$

ℓ being the mean lineal intercept.

Figure 38 indicates how, as heat input of welding increases, the area occupied by sensitized grain boundaries decreases. The grain boundary area is a direct function of the average grain diameter and heat input. It also incorporates the grain boundary area of the as-received and annealed samples. There is a marked difference between the grain

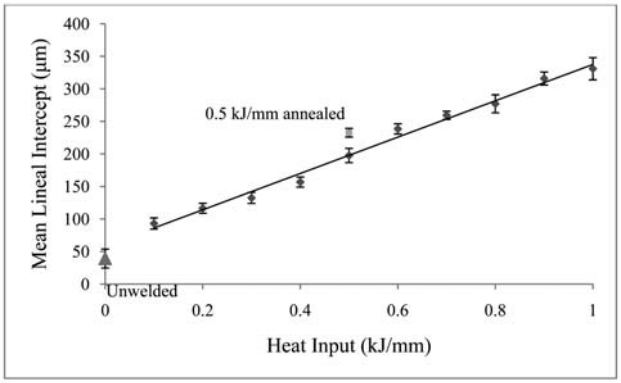

Figure 37—Mean lineal intercept vs. heat input of welding

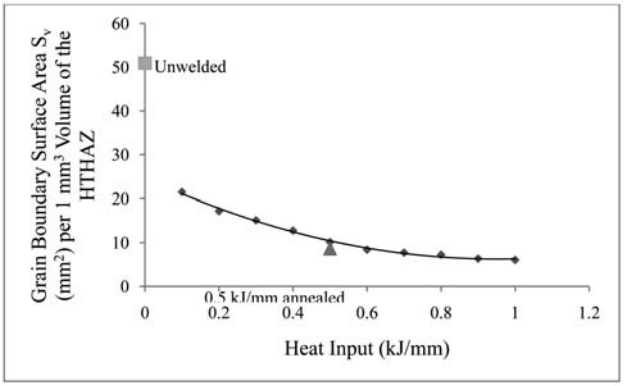

Figure 38—Grain boundary surface area S_v (mm²) per unit volume (1 mm³) of the HTHAZ as a function of the heat input of welding

Table VI

Difference in corrosion, pitting, protection potentials and resistance to pitting corrosion between the as-received and the welded plate in terms of the Ag/AgCl reference electrode

ΔE_{corr} ($V_{Ag/AgCl}$)	ΔE_{pit} ($V_{Ag/AgCl}$)	ΔE_{prot} ($V_{Ag/AgCl}$)	$\Delta(E_{pit} - E_{prot})$ ($V_{Ag/AgCl}$)
0.1	0.395	0.02	-0.33

boundary area of the unwelded (as-received) sample and the grain boundary area of the sample welded at a heat input of 0.1 kJ/mm.

Effect of sensitization on corosion characteristics

Corrosion tests were carried out on the as-received plate and on a sample of the plate welded at 0.4 kJ/mm. Table VI shows the difference in corrosion, pitting and protection potentials between the as-received and welded samples in terms of the Ag/AgCl reference electrode.

For the welded plate, pitting corrosion will start at a lower potential than the unwelded plate, indicating the resistance to pitting corrosion was reduced during welding with 0.395 V. This gives an indication that the welded sample, which was welded in the heat input range where sensitization appeared prolifically, has comparatively poor corrosion characteristics. This can directly be ascribed to the sensitization of the HAZ of the weld.

Conclusions

AISI 409 sensitizes during low heat input welding. For a plate thickness of 2 mm, sensitization occurs for heat inputs of 0.1 to above 0.25 kJ/mm, and for 4 mm plate thickness in the 0.2 to 0.9 kJ/mm heat input range. Due to the faster cooling rate of thicker sections the 4 mm steel experienced sensitization over a much larger heat input range than the 2 mm steel. TiN is stable at temperatures below 1 500°C, therefore there is a decrease in the availability of Ti to form TiC and increased $M_{23}C_6$ precipitation. Rapid cooling through the TiC stability region limits the effectiveness of Ti stabilization. HAZ grain size is directly proportional to the heat input. Annealing at 725°C for 5 minutes does not necessarily improve the sensitization characteristics of the microstructure. After annealing, the weld bead was sensitised and grain boundary ditching and grain dropping was still evident in the heat-affected zone. Due to sensitization pitting corrosion initiates at a lower potential in the welded sample than in the unwelded plate and the resistance to pitting corrosion is reduced during welding.

References

1. CS409—Technical Data. Technical Manual published by Columbus Stainless. 2010.
2. Kim, J.K., Kim, Y.H., Uhmb, S.H., Lee, J.S., and Kim, K.Y. Intergranular corrosion of Ti-stabilized 11 wt% Cr ferritic stainless steel for automotive exhaust systems. Graduate Institute of Ferrous Technology, Pohang University of Science and Technology, Pohang, Korea, 2009.
3. Folkhard, E. *Welding Metallurgy of Stainless Steels*. Springer-Verlag, Vienna, vol. 3, no. 11, 1988, pp. 34–35.
4. Leslie. *The Physical Metallurgy of Steels*. McGraw-HILL, 1983, p. 326, 341.
5. Grobler, C. Weldability studies on 12% and 14% chromium steels. PhD dissertation, University of Pretoria, South Africa, 1987.
6. Kim, J.K., Kim, Y.H., Lee, J.S., and Kim, K.Y. Effect of chromium content on intergranular corrosion and precipitation of Ti-stabilized ferritic stainless steel. Graduate Institute of Ferrous Technology, Pohang University of Sciences and Technology, Pohang, Korea, 2010.
7. Tuling, A. EELS study of sensitization in 12% chromium steel. *Proceedings of the Microscopy Society of Southern Africa* 31, 2001, p. 26.
8. Greeff, M.L. The influence of welding parameters on the sensitization behaviour of 3CR12.MSc thesis. University of Pretoria, South Africa, 2005.
9. Lo, K.H., Shek, C.H., and Lai, J.K.L. Recent developments in stainless steels. University of Hong Kong, Hong Kong, China, 2009.
10. Messler, R.W. Jr. *Principles of Welding*. Wiley-VCH, 2004, pp. 550, 560–561, 563.
11. Williams, J.G., and Barbaro, F.J. Susceptibility and Prevention of Weld HAZ Sensitization and Intergranular Stress Corrosion Cracking in Various 12% Cr steels. *Australasian Welding Journal* vol. 50(4th quarter), 2005, pp. 34–47.
12. Du Toit, M., Van Rooyen, G.T., and Smith, D. An overview of the heat-affected zone sensitization and stress corrosion cracking behaviour of 12% chromium type 1.4003 ferritic stainless steel. *Corrosion,* vol. 63, no. 5, 2005.
13. Van Warmelo, M., Nolan, D., and Norrish, J. Mitigation of sensitization effects in ustabilised 12%Cr ferritic stainless steel welds. Faculty of Engineering, University of Wollongong, Australia, 2007.
14. Greeff, M.L. and Du Toit, M. Looking at the sensitization of 11-12% chromium EN 1.4003 stainless steels during welding. *Welding Journal,* vol. 85, no. 11, 2006, pp. 243s–251s.
15. Easterling, K. *Introduction to the Physical Metallurgy of Welding*. 2nd Edition, Butterworth-Heinemann, 1992, p. 19.
16. ASTM A 763 – 93. Standard Practices for Detecting Susceptibility to Intergranular Attack in Ferritic Stainless Steels. ASTM International, 2004.
17. ASTM E 112 – 96. Standard Test Methods for Determining Average Grain Size. ASTM International, 2004.
18. ASTM G 150 – 99. Standard Test Method for Electrochemical Critical Pitting Temperature Testing of Stainless Steels. ASTM International, 2004.
19. Rosenthal, D. The theory of moving sources of heat and its application to metal treatments. *Transactions of the AIME* 68, 1946, pp. 849–866.
20. Pardo, A., Merino, M.C., Coy, A.E., Viejo, F., Carboneras, M. and Arrabal, R. Influence of Ti, C and N concentration on the intergranular corrosion behaviour of AISI 316Ti and 321 stainless steels. Departamento de Ciencia de Materiales, Facultad de Ciencias Qui´micas, Universidad Complutense de Madrid, Madrid, Spain, 2007. ◆

Sensitization behaviour of 11–12% Cr AISI 409 stainless steel